EPJ Web of Conferences **163**, 00053 (2017) DOI: 10.1051/epjconf/201716300053
FUSION17

Pre-compound emission in low-energy heavy-ion interactions

Manoj Kumar Sharma[1,⋆], Mohd. Shuaib[2], Vijay R. Sharma[3], Abhishek Yadav[3], Pushpendra P. Singh[4], Devendra P. Singh[5], Unnati[6], B. P. Singh[2,⋆⋆], and R. Prasad[2]

[1] *Department of Physics, Sri Varsheny (Post Graduate) College, Aligarh (UP) - 202 001, India*
[2] *Department of Physics, Aligarh Muslim University, Aligarh 202 002, India*
[3] *NP-Group, Inter University Accelerator Centre, New Delhi - 110 067, India*
[4] *Department of Physics, Indian Institute of Technology Ropar, Punjab 140 001, India*
[5] *Department of Physics, University of Petroleum and Energy Studies, Dehradun - 248 007, India*
[6] *Department of Physics and Astrophysics, Delhi University, Delhi-110007 India*

Abstract. Recent experimental studies have shown the presence of pre-compound emission component in heavy ion reactions at low projectile energy ranging from 4 to 7 MeV/nucleons. In earlier measurements strength of the pre-compound component has been estimated from the difference in forward-backward distributions of emitted particles. Present measurement is a part of an ongoing program on the study of reaction dynamics of heavy ion interactions at low energies aimed at investigating the effect of momentum transfer in compound, pre-compound, complete and incomplete fusion processes in heavy ion reactions. In the present work on the basis of momentum transfer the measurement of the recoil range distributions of heavy residues has been used to decipher the components of compound and pre-compound emission processes in the fusion of ^{16}O projectile with ^{159}Tb and ^{169}Tm targets. The analysis of recoil range distribution measurements show two distinct linear momentum transfer components corresponding to pre-compound and compound nucleus processes are involved. In order to obtain the mean input angular momentum associated with compound and pre-compound emission processes, an online measurement of the spin distributions of the residues has been performed. The analysis of spin distribution indicate that the mean input angular momentum associated with pre-compound products is found to be relatively lower than that associated with compound nucleus process. The pre-compound components obtained from the present analysis are consistent with those obtained from the analysis of excitation functions.

1 Introduction

The pre-compound (PCN) emission process in heavy ion reactions at relatively low energies ranging from 4 to 7 MeV/nucleon has been a topic of recent interest [1], since it is, generally, expected to occur at relatively high energies ≈10-15 MeV/nucleon[2]. The PCN process may be understood as the fusion of two heavy nuclei in such a way so that a composite nucleus forms far from the statistical equilibrium, and a large fraction of its energy is considered to be in the form of an orderly translational motion of the nucleons of the projectile and target nucleus[3–8]. This orderly motion transforms slowly into chaotic thermal motion through a series of two-body interactions. The thermalization process completes when the composite nucleus reaches a state of thermal equilibrium referred to as compound nucleus (CN). During the thermalization of an excited composite system, it may be possible that a single nucleon or a cluster of nucleons having considerable energy is ejected into the continuum. As soon as the state of thermal equilibrium is attained, the accumulation of sufficient energy on a single nucleon or a cluster of nucleons may occur in a random sequence of events and hence, may require much longer emission times favoring the emission of low energy particles. The emission of such light particles prior to the establishment of thermodynamic equilibrium of the composite system are termed as the PCN particles and the reaction mechanism is referred to as the PCN process.

The time scale at which PCN emissions occur is very short $\approx 10^{-21}$ sec., while for further evaporations from the equilibrated nucleus take a longer time $\approx 10^{-16}$ sec. The rate of emission of the PCN nucleons depends on the complexity of self-consistent mean-field interaction between the projectile and target nucleus, their structure effects[7, 9] and excitation energy availed by nucleons of composite system. This determines the initial energy distribution among the nucleons in the projectile and the target nuclei, which starts a cascade of nucleon-nucleon interactions as soon as the two nuclei touch each other. Some of the important experimental characteristics of the PCN process are; (i) the presence of a larger number of high-energy particles as compared to the spectrum predicted by the statistical model, (ii) forward-peaked angular distribution of the emitted particles through PCN process, (iii) ob-

⋆ e-mail: manojamu76@gmail.com
⋆⋆ e-mail: bpsinghamu@gmail.com

servation of smaller recoil range/linear momentum of the evaporation residues left over emission of PCN particles as compared to CN particles, (iv) observation of lower value of the spin with PCN process as compared to CN process, (v) slowly decreasing tails of the excitation functions (EFs) etc.,

In the earlier measurements, the relative strengths of the PCN and CN components in the reactions were estimated from the enhancement in the flux of emitted light particles in the forward direction over the backward direction. The other method often employed is to analyze the measured EFs of evaporation residues by comparing with the statistical model predictions. The observed deviation in EFs with statistical model predictions at relatively higher projectile energies side (tail portion of the EFs) is attributed to the PCN emission process. During last few decades the understanding of the PCN and the CN emission in light ion reactions has been well studied but in heavy ion reactions it needs to be further explored particularly for those associated with the emission of light particles in primary stage in a very short reaction time (10^{-21} s) prior to the establishment of equilibrated CN[7, 10–14]. The emission of such PCN particles reduces the momentum of the product residues. As such, the measurements of the momentum transfer during the interaction may provide a promising tool for the characterization of the reaction mechanism involved.

Although, information about the momentum transfer in heavy ion reaction may also be obtained by several methods[2, 15, 16], in the present measurements this information has been obtained from the study of the recoil range distributions (RRDs) and the spin distributions (SDs) of the reaction residues. Since emitted PCN particles takes away a significant part of angular momentum as compared to CN particles, the angular momentum associated with the PCN products is relatively lower than that associated with the CN process. Therefore, in PCN reactions, the residues are populated at relatively lower spin states as compared to those of the residues populated via CN process. This paper is organized as follows. The experimental details and analysis of RRDs, SDs and EFs are given in the subsections of the section 2. The conclusions drawn from the analysis are given in the section 3 of this paper.

2 Experimental details and analysis

In the present paper the following three self-consistent measurements i.e., (i) the recoil range distributions (RRDs), (ii) the spin distributions (SDs) of the product nuclei and (iii) the excitation functions (EFs), have been performed in the interaction of ^{16}O projectile with ^{159}Tb and ^{169}Tm targets. In both RRDs and EFs measurements, the detection of delayed γ-rays of product residues takes place through the recoil catcher off-line spectroscopy based activation technique. However, the measurements of the SDs is based on the detection of prompt γ-rays of product residues in a particle-γ coincidence experiments in forward and backward directions. A brief description on each experiment carried out in the Inter University Accelerator

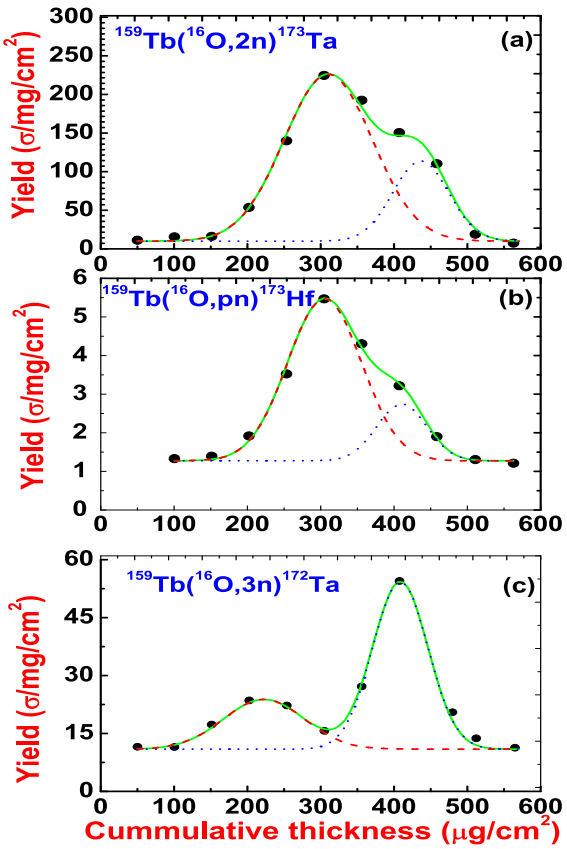

Figure 1. (Color online) The experimentally measured RRDs for the reactions ^{159}Tb(^{16}O,2n)^{173}Ta, ^{159}Tb(^{16}O,pn)^{173}Hf and ^{159}Tb(^{16}O,3n)^{172}Ta at energy ≈90 MeV. In this figure a Gaussian peak (blue dotted curve) obtained from ORIGIN software at higher cumulative thickness represents CN contribution while other Gaussian (red dashed curve) at lower thickness represents PCN contribution.

Centre (IUAC), New Delhi, India along with their results are given in following subsections;

2.1 Measurement and Analysis of Recoil Range Distributions

In order to investigate the role of linear momentum transfer in the PCN emission, the experiments have been carried out at in the General Purpose Scattering Chamber (GPSC) of IUAC, New Delhi, India to measure the RRDs of recoiling residues produced both by the CN and the PCN emission processes in the reactions ^{159}Tb (^{16}O,2n) ^{173}Ta, ^{159}Tb (^{16}O,pn) ^{173}Hf and ^{159}Tb(^{16}O,3n)^{172}Ta for the ^{16}O+^{159}Tb system at 90 MeV and for reactions ^{169}Tm(^{16}O, 2n)^{183}Ir and ^{169}Tm(^{16}O, 3n)^{182}Ir in the ^{16}O+^{169}Tm system at incident energy 88 MeV, respectively. The Coulomb barrier for systems ^{16}O+^{159}Tb and ^{16}O+^{169}Tm are ≈ 64 and 67 MeV respectively. In this experiment, the target (thickness ≈ 500 $\mu g/cm^2$ for ^{169}Tm and ≈ 400 $\mu g/cm^2$ for ^{159}Tb) followed by a stack of nearly fifteen thin Al catcher foils of varying thickness (≈ 16-45 $\mu g/cm^2$ prepared by vacuum evaporation technique) was mounted in the GPSC

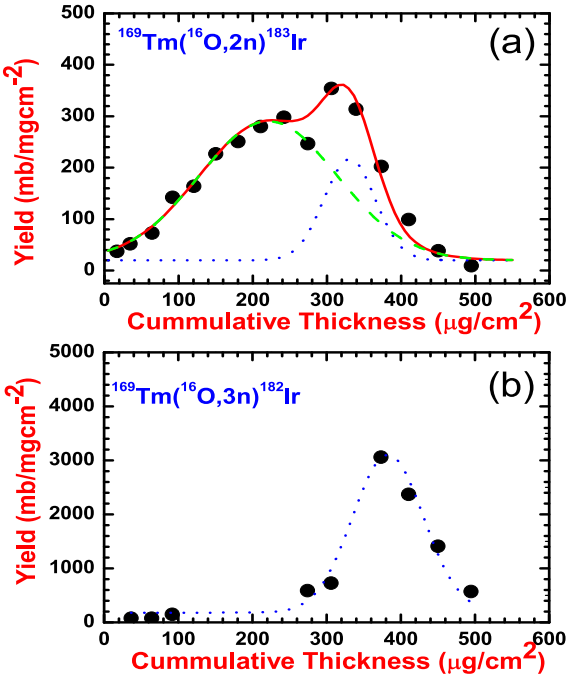

Figure 2. (Color online) (a-c). The experimental RRD for the reactions ^{169}Tm(^{16}O,2n)^{183}Ir and ^{169}Tm(^{16}O,3n)^{182}Ir at energy ≈88 MeV. In this figure a Gaussian peak (blue dotted curve) at higher cumulative thickness represents CN contribution while other Gaussian (red dashed curve) at lower thickness represents PCN contribution.

normal to the beam direction. Furthermore, SRIM[17] calculations of energy loss in the target sample has been performed to calculate the energy of recoiling residues at the mid of the target. Depending on the momentum carried away by the product residues, the recoiling residues were trapped at different ranges in the stack of thin Al-foils. The duration of irradiation was about 15 hrs. The thickness of the catcher foils was measured precisely prior to their use, by measuring the energy loss suffered in each catcher foil by 5.485 MeV α particles from ^{241}Am source. The code SRIM[17] was used for determining the thickness from the energy loss measurements.

The activities induced in each thin catcher were followed off-line for about two weeks using a pre-calibrated high resolution (2 keV for 1.33 MeV γ ray of ^{60}Co) HPGe detector. The experimental cross-section (σ) for the reaction products in different catcher foils were divided by its respective thickness that gives the resulting yield of experimentally measured RRDs. The experimental uncertainties in cross-section is <10% that arise due to various factors viz., uncertainty in the number of target nuclei due to non-uniformity in sample thickness, the fluctuations in the beam current, uncertainty in the determination of detector efficiency, statistical error in counts and the dead time of the counting system. The experimentally measured RRDs for reactions ^{159}Tb(^{16}O,2n)^{173}Ta, ^{159}Tb(^{16}O,pn)^{173}Hf and ^{159}Tb(^{16}O,3n)^{172}Ta at 90 MeV are shown in Fig 1 (a-c). Solid curve in this figure guides the eye to the experimental RRD data. As can be seen from this figure that the experimental RRD data for these reactions has two peaks, one at a relatively lower value (≈ 250-300$\mu g/cm^2$, depending on straggling and number of evaporation residues) of cumulative catcher thickness and the other at ≈ 400-450 $\mu g/cm^2$. The peak at ≈ 400-450 $\mu g/cm^2$ corresponds to the fraction of residue produced through the CN process and is consistent with the full momentum transfer events in complete fusion reactions. The peak at relatively smaller range may be attributed to the fact that the residues ^{183}Ir are produced via the PCN process when emission of neutrons takes place prior to the establishment of thermodynamical equilibrium. The theoretical value (mean range) of the experimental RRD data is calculated with the help of energy loss program of the code SRIM and this value of mean range is fed in the program ORIGIN to fit the Gaussian peak of the experimental RRD. The Gaussian peak (shown by red dashed curve) at lower cumulative catcher thickness of larger width is obtained which shows the contribution of PCN emission. By using similar procedure, the RRDs for reactions ^{169}Tm(^{16}O,2n)^{183}Ir and ^{169}Tm(^{16}O,3n)^{182}Ir have also been measured at ≈88 MeV. The experimental RRDs with their theoretical simulations for these reactions are shown in Fig 2 (a-b), respectively. The peaks in the experimental RRD arise due to the overlap of the heavy residues produced via two different reaction mechanism i.e, the CN and the PCN emission of particles. As can be seen from this figure that the experimental RRD data for the reaction ^{169}Tm(^{16}O,2n)^{183}Ir has two peaks, one at a relatively lower value (≈ 200-250$\mu g/cm^2$) of cumulative catcher thickness and the other at ≈ 330-380 $\mu g/cm^2$. The peak at ≈ 330-380 $\mu g/cm^2$ corresponds to the fraction of residue produced through the CN process. It is pointed out here that due to short half live(≈15 min) of the residue ^{182}Ir, we could measure only the RRD corresponds to CN component.

2.2 Measurement and Analysis of Spin Distributions

The second experiment based on particle-gamma coincidence technique has been performed for measuring the population of spin states during de-excitation of reaction residues. In the present work, the spin-distributions of the reaction ^{159}Tb(^{16}O,2n)^{173}Ta at ≈93 MeV and for ^{169}Tm(^{16}O,2n)^{183}Ir at ≈88 MeV have been measured using Gamma Detector Array (GDA) alongwith Charged Particle Detector Array (CPDA). The Experimental details are given in Ref. [21]. However, we mention them here in brief for ready reference. The GDA is an assembly of 12 Compton suppressed, high resolution HPGe γ-spectrometers arranged at 45^0, 99^0, and 153^0 angles with respect to the beam axis and there are four detectors at each of these angles. The CPDA is a set of 14-phoswich detectors housed in a 14 cm diameter scattering chamber, covering nearly 90% of total solid angle. The reaction residues have been identified from their characteristic prompt γ-transition lines [22]. The values of relative production yields of the residues (observed area under the peak of the experimentally measured prompt gamma

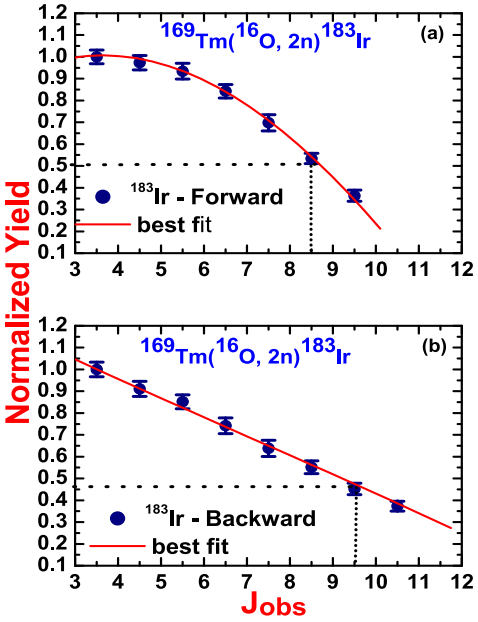

Figure 3. (Color online) The experimentally measured spin distributions for reactions ^{169}Tm(^{16}O,2n)^{183}Ir in forward and backward directions. The curve and line in this figure guide the eye as a best fit to the experimentally normalized yield of spin distributions of PCN and CN processes.

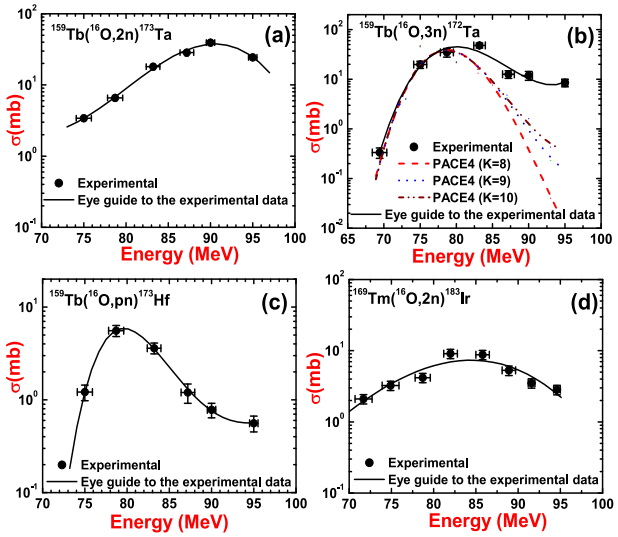

Figure 4. (Color online) (a-d) The experimentally measured EFs for reactions ^{159}Tb(^{16}O,2n)^{173}Ta, ^{159}Tb(^{16}O,pn)^{173}Hf, ^{159}Tb(^{16}O,3n)^{172}Ta, and ^{169}Tm(^{16}O,2n)^{183}Ir, respectively. The theoretically calculated EFs by using code PACE4 gives negligibly small values of cross-sections for all these reactions except for ^{159}Tb(^{16}O,3n)^{172}Ta. The experimentally measured EFs and the PACE4 predictions with different values of parameter K from K=8 to K=10 for reaction ^{159}Tb(^{16}O,3n)^{172}Ta is also shown in Fig 4(b).

lines with proper detector efficiency correction) have been plotted as a function of observed spin J_{obs} corresponding to prompt gamma-transitions[23]. The relative yield has been normalized with minimum observed spin (J^{min}_{obs}) at highest yield (Y^{max}_{obs}). As a representative case the experimentally measured SDs obtained from prompt γ-rays recorded in forward and backward directions for the reaction ^{169}Tm(^{16}O,2n)^{183}Ir are shown in Fig 3 (a) and 3(b) at 88 MeV, respectively. As can be seen from these figures, the measured SD and hence its decay pattern for this reaction obtained in the forward and backward directions are distinctly different from each other indicating widely different reaction mechanisms involved. It may be pointed out the entirely different shapes of SDs in forward and backward directions indicate that the two processes are quite different in nature.

The observed lower value of the mean input angular momentum ($\approx 8.5\hbar$) in forward direction is due to the fact that emission of two PCN neutrons takes away a significant part of the angular momenta. On the other hand a relatively higher observed value of the mean input angular momentum in backward direction ($\approx 11.5\hbar$) is because of the emission of two equilibrated neutrons. As such, it is concluded that distinctly different SDs give a direct evidence of the PCN emission process. Thus, the results of the measurements of the SDs further supplement the conclusions drawn from the RRDs measurements.

2.3 Measurement and Analysis of Excitation Functions

The thirds experiment has been carried out for measuring the EFs by using stacked foil activation technique. In this experiment the stacks consisting of (^{159}Tb and ^{169}Tm) target samples followed by Al foils of suitable thickness have been irradiated for ≈8-10 h in a GPSC of 1.5 m diameter having an in-vacuum transfer facility. The Al foils serve as energy degrader as well as catcher foil where the recoiling residues are trapped. The pertinent decay data required for cross-section measurements of the reaction residue has been taken from Ref.[24]. The activities produced in each target catcher assembly have been measured using a high resolution large volume (100 c.c.) High Purity Germanium Detector (HPGe). The reaction cross sections for the product residues have been obtained from the measured intensities of the characteristic γ-rays using the standard formulation[1].

The analysis of experimental EFs has been performed within the framework of statistical model calculations based on code PACE4[25] that calculates the reaction cross-section for evaporation residues (not for pre-compound residues) using the Bass formula[26]. The level density used in this code is calculated from the expression $a = (A/K)$, where, A is the mass number of the compound nucleus and K is a free parameter known as level density parameter constant. The experimentally measured EFs for the reactions ^{159}Tb(^{16}O,2n)^{173}Ta, ^{159}Tb(^{16}O,3n)^{172}Ta,

^{159}Tb(^{16}O,pn)^{173}Hf and ^{169}Tm(^{16}O,2n)^{183}Ir in the energy range ≈70-95 MeV are shown in Figs. 4 (a) to 4(d), respectively. The half-lives of these evaporation residues ^{173}Ta, ^{172}, ^{173}Hf and ^{183}Ir are 3.14 h, 36.8 m, 23.6 h and 57 m, respectively. The solid curves in these figures guide to the eye to the experimentally measured EFs. The theoretically calculated EFs by using code PACE4 gives negligibly small values of cross-sections for all these reactions except ^{159}Tb(^{16}O,3n)^{172}Ta, hence, the cross-section values obtained from code PACE4 are not shown in figures 4(a), 4(c) and 4(d). In the present calculations, the effect of variation of parameter K from K=8 to K=10 of code PACE4 on measured EFs for reaction ^{159}Tb(^{16}O,3n)^{172}Ta is also shown in Fig. 4(b). As can be seen from this figure, by varying the value of K, the experimentally measured EFs could not be reproduced in higher energies (tail portion of EFs) side. The higher values of experimental cross sections in the tail portion of EFs for this reaction as compared to the theoretical calculations may be attributed to the PCN emission process, which is one of the dominant mode reaction channels and is not considered in the PACE4 calculations. It means that analysis of EFs with code PACE4 gives negligible contribution of CN process for the reactions ^{159}Tb(^{16}O,2n)^{173}Ta, ^{159}Tb(^{16}O,pn)^{173}Hf and ^{169}Tm(^{16}O,2n)^{183}Ir , while the analysis of RRD for the same reactions gives energy dependent contributions of the CN and the PCN processes. This shows that RRD measurements are much sensitive as compared to those of EFs. The analysis of measured EFs for reaction ^{169}Tm(^{16}O,3n)^{182}Ir gives a contribution of ≈35% PCN and ≈65% of CN at ≈88 MeV as shown in Fig 4 (b). This data is consistent with the corresponding values obtained from the RRD measurements at ≈88 MeV. Further, the reasonable agreement between the two sets of experiments speaks favorably on the consistency of these measurements.

3 Conclusions

The significant contribution due to PCN process has been observed. The results obtained by RRDs are supported by the SD measurements. The RRD measurements are found to be sensitive tool to decipher the CN and the PCN processes. The auxiliary experiments on the EF measurements is found to be consistent with both the RRD and SD measurements.

4 Acknowledgements

The authors are thankful to the Director, IUAC, New Delhi for extending all the facilities for carrying out the experiments. MKS thanks to the Council of Scientific and Industrial Research (CSIR), New Delhi, India vide the project number 03(1361)16/EMR-11 for financial support.

References

[1] M. K. Sharma, P. P. Singh, D. P. Singh, V. Sharma, A. Yadav, Unnati, Indu Bala, R. Kumar, B. P. Singh, and R. Prasad, Phys. Rev. C **91**, 044601 (2015).
[2] J. Gómez del Campo, D. Shapira, J. McConnell, C. J. Gross, D. W. Stracener, H. Madani, E. Chávez, M. E. Ortíz, Phys. Rev. C **60R**, 021601 (1999).
[3] M. Blann, Ann. Nucl. Sci. **25**, 123 (1975).
[4] M. Blann Nucl. Phys. A **235**, 211 (1974).
[5] E. Holub, D. Hilscher, G. Ingold, U. Jahnke, H. Orf, and H. Rossner, Phys. Rev. C **28**, 252 (1983).
[6] E. Holub, D. Hilscher, G. Ingold, U. Jahnke, H. Orf, H. Rossner, W. P. Zank, W. U. Scroder, H. Germeke, K. Keller, L. Lassen, and W. Lucking, Phys. Rev. C **33**, 143 (1986).
[7] M. Cavinato, E. Fabrici, E. Gadioli, E. Gadioli Erba, P. Vergani, M. Crippa, G. Colombo, L . Redaelli, and M. Ripamonti, Phys. Rev. C **52**, 2577 (1995).
[8] F. Amorini, M. Cabibbo, G. Cardelaa, A. Di Pietro, A. Musumarra, M. Papa, G. Pappalardo, F. Rizzo, and S. Tudisco, Phy. Rev. C **58**, 987 (1988).
[9] H. Zheng, S. Burrello, M. Colonna and V. Baran, Phys. Lett. B **769**, 424 (2017).
[10] H.C. Britt and A.R. Quinton, Phys. Rev. **124**, 877 (1961).
[11] T. Otsuka and K. Haradav, Phys. Lett. B **121**, 106 (1983).
[12] P. Vergani, E. Gadioli, E. Vaciago, E. Fabrici, E. Gadioli Erba, M. Galmarini, G. Ciavola, and C. Marchetta, Phys. Rev. C **48**, 1815 (1993).
[13] C. Birattari et. al, Phys. Rev. C **54**, 3051 (1996).
[14] H. Delagrance, A. Fleury, F. Hubert, and G. N. Simonoff, Phys. Lett. B **37**, 397 (1971).
[15] H. Morgenstern, W. Bohne, K. Grabisch, D. G. Kover and H. Lehr, Phys. Lett. B **113**, 463 (1982).
[16] B. B. Back et. al., Phys. Rev. Lett. **50**, 88 (1983).
[17] The Stopping and Range of Ions in Matter (SRIM) code: [http://www.srim.org/SRIM/SRIMLEGL.htm].
[18] M. K. Sharma et. al., Phys. Rev. C **70**, 044606 (2004).
[19] D. P. Singh et. al, Phys. Rev. C **81**, 054607 (2010).
[20] M. K. Sharma et. al., Phys. Rev. C **91**, 024606 (2015).
[21] P. P. Singh, B. P. Singh, M. K. Sharma et al., Phys. Lett. B 671, 20 (2009).
[22] S. Andrd, J. Genevey-Rivier, et al., Phys. Rev. Lett. 38, 327 (1977).
[23] RADWARE Level Scheme http://radware.phy.ornl.gov/agsdir1.html.
[24] E. Browne and R. B. Firestone, 1986 Table of Radioactive Isotopes (Wiley, New York).
[25] A. Gavron, Phys. Rev. C **21**, 230 (1980).
[26] R . Bass, Nucl. Phys. A **231**, 45 (1974).